ELSEVIER

Journal of Power Sources 81–82 (1999) 458–462

JOURNAL OF POWER SOURCES

www.elsevier.com/locate/jpowsour

Characteristics of the 4 V plateau in $LiMn_2(O_{4-x}F_x)$ studied by in situ synchrotron X-ray diffraction

P. Strobel [a,*], M. Anne [a], Y. Chabre [b], M.R. Palacín [c,d], L. Seguin [c], G. Vaughan [e], G. Amatucci [f], J.M. Tarascon [c]

[a] *Laboratoire de Cristallographie CNRS, BP 166, 38042 Grenoble cedex 9, France*
[b] *Laboratoire de Spectrométrie Physique UJF-CNRS, BP 87, 38402 St. Martin d'Hères cedex, France*
[c] *Laboratoire de Réactivité et Chimie des Solides, Univ. de Picardie and CNRS, 80039, Amiens cedex, France*
[d] *Institut de Ciència de Materials, CSIC, 08193 Bellaterra, Spain*
[e] *ESRF, BP 220, 38043 Grenoble cedex, France*
[f] *Bellcore Research, Red Bank, NJ 07701, USA*

Abstract

Fluorine-substituted $Li_xMn_2O_4$ was studied by synchrotron X-ray diffraction using Bellcore-type plastic batteries placed directly in the synchrotron beam. The results show that the '4 V plateau' actually contains three regions: (1) a single-phase range for $0.59 \leq x \leq 1$, (2) a two-phase range for $0.23 \leq x \leq 0.59$, (3) a narrow single-phase range for $x \leq 0.23$. These three domains are fully reversible, but the plastic battery undergoes extraneous oxidation reactions for voltages ≥ 4.4 V. The structural features of this compound are qualitatively similar to those of stoichiometric $Li_xMn_2O_4$. In particular, no suppression of the two-phase range such as that observed on non-stoichiometric or Ni-substituted $LiMn_2O_4$ was found. © 1999 Elsevier Science S.A. All rights reserved.

Keywords: Lithium-ion batteries; Manganese oxide; Diffraction; Synchrotron

1. Introduction

The spinel phase $LiMn_2O_4$ is one of the best currently available materials for rocking-chair rechargeable batteries. The extraction of lithium from stoichiometric $LiMn_2O_4$ occurs at ca. 4 V vs. Li/Li^+ and leads to cation-vacant spinels $Li_xMn_2O_4$ with $0 \leq x \leq 1$. This material does not perform as well as rhombohedral ABO_2 oxides such as $LiCoO_2$ or $LiNiO_2$, but it has important advantages in terms of cost and environmental aspects [1]. Its properties can also be modified by stoichiometry changes in the highly versatile spinel structure.

Previous reports about the structural features of the electrochemical lithium extraction from $LiMn_2O_4$ agree about the existence of two slightly different plateaux in $U(x)$ at 4.0 and 4.1 V [2–7]. However, some discrepancies exist about the extent of these two oxidation steps and about their single-phase or two-phase nature. These actually depend on the initial spinel composition, as shown by several authors [4–7].

We investigate here new compositions recently proposed by the Bellcore group, i.e., fluorine-substituted spinel. The development of plastic batteries by Bellcore [8] allows to perform X-ray diffraction experiments in transmission directly through complete battery packages. The present paper describes such a combined electrochemical and structural study achieved by in situ diffraction using synchrotron radiation.

2. Experimental

The preparation of fluorine-doped $LiMn_2O_4$ is described elsewhere [9]. The determination of its Mn oxidation state yields $\nu(Mn) \approx 3.40$, corresponding to the formula $LiMn_2(O_{3.8}F_{0.2})$. The electrolyte used was 1 M $LiPF_6$ in EC:DMC (2:1 v/v). The cells were monitored using a MacPile controller (Bio-Logic, Claix, France).

The angular domain was -8 to $+48°$ in 2θ, for a wavelength of 0.40 Å. The counting time was ca. 22 m/scan. The cell, containing 406 mg active material, was cycled under pseudo-galvanostatic control over a charge–discharge cycle between 3.9 and 4.7 V in ca. 32 h,

* Corresponding author. Tel.: +33-4-7688-7940; Fax: +33-4-7688-1038; E-mail: strobel@labs.polycnrs-gre.fr

0378-7753/99/$ - see front matter © 1999 Elsevier Science S.A. All rights reserved.
PII: S0378-7753(98)00222-5

allowing to record more than 80 high-resolution diffraction patterns over this cycle. The details of diffractometer set-up and data collection are described elsewhere [10].

3. Results and discussion

The first pattern recorded on the electrochemical cell cycled in situ is shown in Fig. 1. Diffracting in transmission mode through complete flat plastic batteries in the beam yielded Bragg reflections from the positive electrode oxide, the current collectors (aluminum and copper grids), as well as a few weak reflections due to graphite and LiC_n at rather low angle. As shown in Fig. 1, both aluminum and copper give intense and sharp lines, which can be used as internal standards throughout the experiment. The oxide reflections are also very well defined: the linewidths at mid-height for these three phases lie in the range 0.02–0.03 at $2\theta \approx 10°$ and 0.035 at 19–20°.

A close examination of the pattern in Fig. 1 shows the occurrence of a slight splitting of most spinel reflections into three components (see for instance lines at $2\theta = 11.0$ (400) and 14.5 (511). This phenomenon disappears at the beginning of charge. It is ascribed to the presence of an orthorhombically-distorted spinel in the initial material; this issue is addressed in detail elsewhere [11].

The evolution of the diffraction pattern along a charge–discharge cycle is shown in Fig. 2. Note first the constant line at $2\theta = 16.07$, due to the aluminum grid collector. The position of this line was constant within $\pm 0.001°$ throughout the whole cycling (ca. 32 h), which gives a good idea of the resolution and accuracy of the diffractometer. In the angular range displayed in Fig. 2, spinel lines occur at ca. 14.6, 15.9 and 16.6° 2θ, corresponding to reflections (511 + 333), 440 and 531, respectively.

Starting from the bottom of Fig. 2a (charge), we observe first a constant increase in angular position with decreasing lithium content to $x \approx 0.48$. At this point, a second line at larger angles starts to emerge and the following of the charge is reflected mostly in a progressive increase in the intensity of this second set of reflections, while the initial set decreases and vanishes at $x \approx 0.25$. This is particularly visible for the 440 reflection which has an initial component on the left of the Al line and a 2nd-phase component on the right of the Al line. Fig. 2b, corresponding to the subsequent discharge, shows that these features are reversible: the strong 440 line at $2\theta = 16.2$, for instance, decreases in intensity and finally vanishes while the corresponding line below the aluminum one grows again. From the evolution of this peak at $2\theta \approx 15.9$, one notes that its angular position is very constant for $0.24 \leq x \leq 0.48$.

A final comment on Fig. 2 is the very noticeable broadening of the spinel reflections towards the end of the charge–discharge cycle (see upper part of Fig. 2b).

These data were analyzed using a full pattern matching refinement procedure. The evolution of refined cell parameters as a function of lithium content x (see Fig. 3) shows three main regions: a single-phase range with variable lattice parameter at high x values, a two-phase range and perhaps a second single-phase range at low x values (see Fig. 3). We note, however, a systematic shift in x between data collected on charge and on discharge. This can be seen very clearly in the upper single-phase range ($8.16 < x < 8.23$) as well as for phases with a $\lesssim 8.09$. The difference in x between both sets of data is roughly constant and corresponds to a 'loss' of ca. $0.10\,x$ between charge and discharge.

Focusing now on the end of the charge (left part of Fig. 3), one notices that a capacity of 0.08 in x was observed

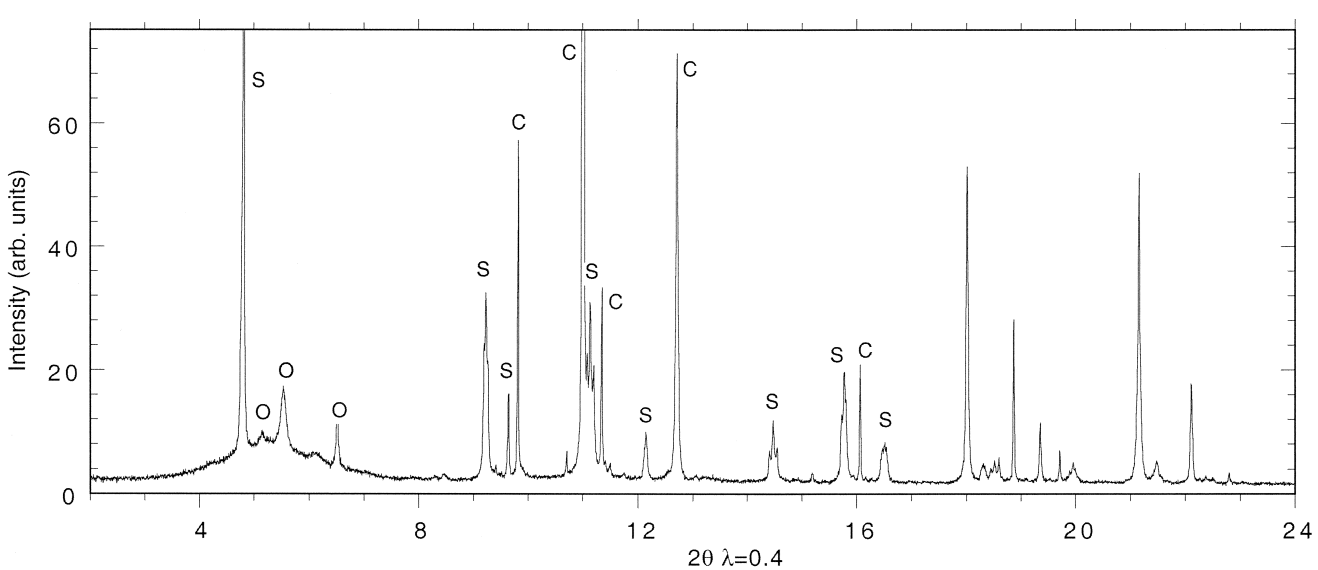

Fig. 1. Synchrotron X-ray powder pattern of $LiMn_2(O_{4-y}F_y)$ recorded in situ on a Bellcore plastic battery equilibrated at 3.27 V. S = spinel reflection, C = collector material reflection (Al, Cu), and O = reflections due to other components.

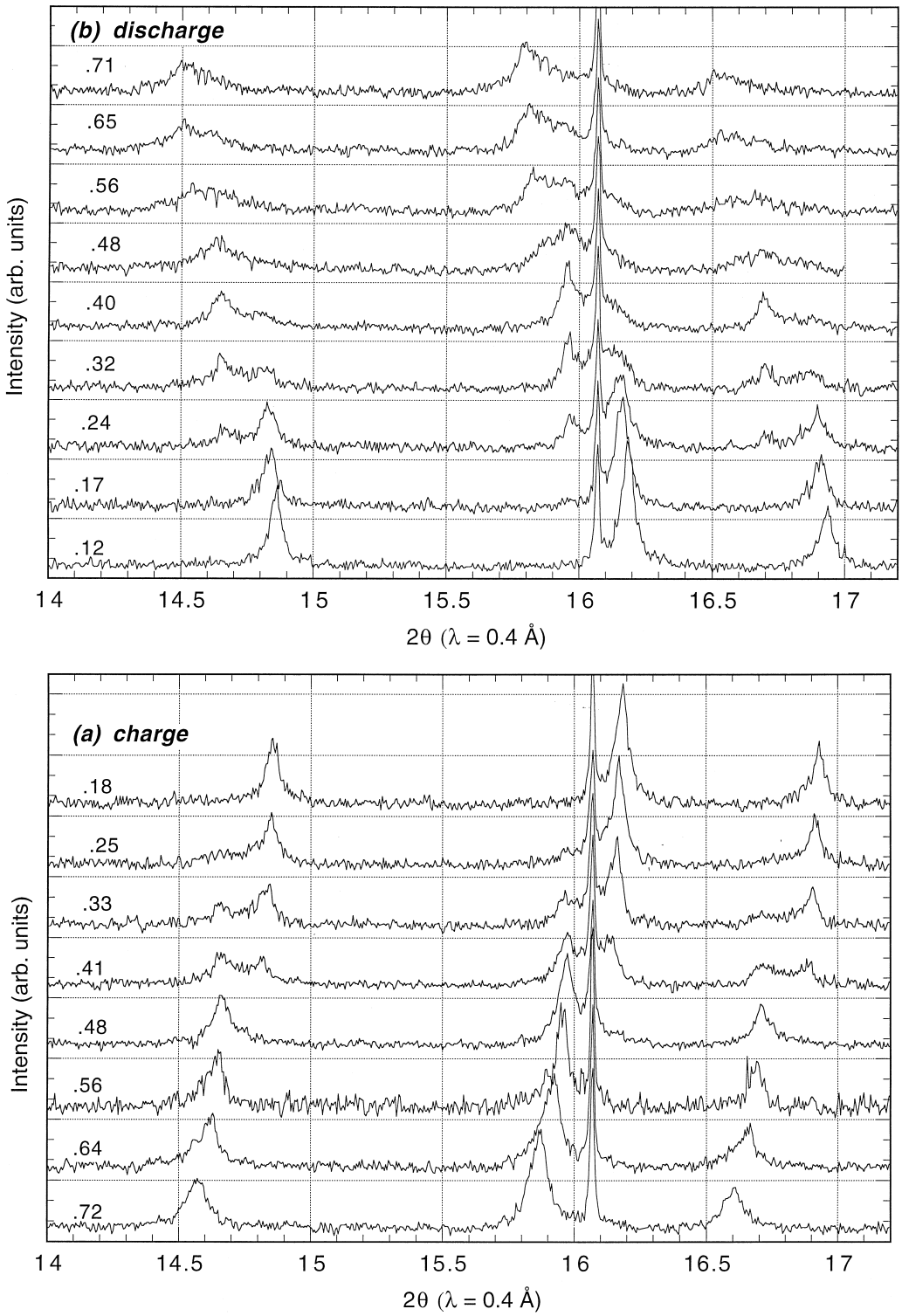

Fig. 2. Evolution of the synchrotron X-ray powder pattern of $Li_xMn_2(O_{4-y}F_y)$. recorded in situ over a charge–discharge cycle (bottom to top). Values of x are indicated on the scans. (a) Charge from 3.95 to 4.7 V; (b) discharge to 3.92 V.

on charge above 4.4 V. But $U(x)$ decreased very abruptly on the subsequent discharge and this capacity was not recovered (Δx[discharge, 4.7 → 4.4 V] = 0.011 only). All this evidence shows that the shift in x-scale between charge and discharge data is likely to be due to extraneous irreversible reactions at high potential, like partial electrolyte oxidation. Such reactions consume electrical capacity and artificially alter the x-scale. The number and

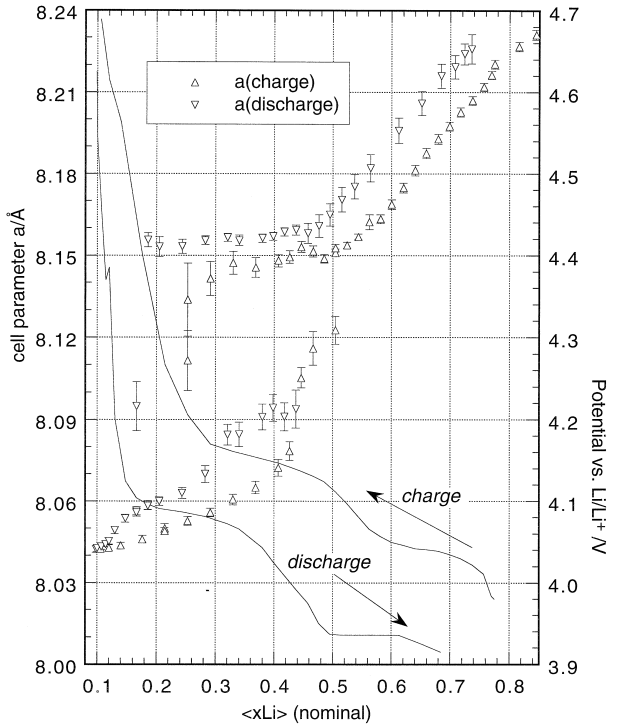

Fig. 3. Evolution of potential and spinel lattice parameter along a pseudo-galvanostatic charge–discharge cycle in $Li_xMn_2(O_{4-y}F_y)$.

quality of the data in the upper single-phase range allowed us to calculate accurately this shift in order to bring the lattice parameter values in coincidence. The value obtained is $\Delta x = 0.080 \pm 0.001$.

The cell parameters vary linearly with lithium content in the range $0.55 \leq x \leq = 0.85$, following the relationship:

$$a/\mathring{A} = 8.0112 + 0.266\,x. \quad (1)$$

A transition from single-phase to two-phase lithium deintercalation occurs at $x \approx 0.55$. It is also clearly visible in the $U(x)$ curve, which presents an inflexion point at $x \approx 0.54$ on both charge and discharge.

The two-phase range extends from $x = 0.55$ to $x \approx 0.25$. The lattice parameter for the upper-*a* phase is very constant in this range: the data obtained on charge all fit the value 8.156 ± 0.003 Å (11 values refined). The data obtained on charge are somewhat lower and more scattered, probably because of a difference in kinetics on reversal of the upper-*a* phase ↔ lower-*a* phase transformation. The presence of extremely constant aluminum and copper reflections (see Fig. 2) shows that this effect is not due to a zero or other geometrical shift.

The lattice parameter of the lower-*a* phase is found to vary continuously during the two-phase process, on both charge and discharge. It seems that not only the fractions of the two oxide phases, but also the composition of the lower-*a* one changes in this range. This may again reflect kinetic limits: we note that the $U(x)$ variation is not flat in this composition range.

As for the upper-*x* limit of the two-phase range, a very good correspondence is observed between structural and electrochemical features at the lower-*x* end: the disappearance of the upper-*a* phase corresponds to a rather abrupt increase in potential.

Regarding the $x < 0.25$ range, a significant increase in slope of the $a = f(x)$ variation down to $x = 0.18$ with respect to the neighbouring data points can be noticed. This trend is supported by numerous and accurate data points, and it can be regarded as the signature of a narrow but actual single-phase intercalation range.

On the contrary, the variation in a is negligible for $x < \approx 0.18$. This corresponds precisely to voltages ≥ 4.4 V, where the change in capacity is attributed to other reactions. In fact, the onset of constant a parameter is a way of locating the end of the lithium extraction reaction, namely $x = 0.18 \pm 0.01$. All points at $x(\text{nominal}) < 0.18$ probably correspond to the same $Li_{0.18}Mn_2(O_{4-y}F_y)$ phase, with $a = 8.0428 \pm 0.005$ Å. Finally, note that the absence of a variation in the range $0.10 \leq x \leq 0.18$ yields an extraneous irreversible capacity $\Delta x = 0.08$, in excellent agreement with that deduced from the apparent shift in $a = f(x)$ curves in the upper single-phase range (see above).

4. Conclusions

This experiment very clearly showed the structural features of the 4 V charge–discharge plateau in fluorine-substituted $LiMn_2O_4$. The general characteristics are rather similar to those of stoichiometric $LiMn_2O_4$. Some scattering exists about the two-phase range limits among various authors [2–7], which may be due to differences in electrochemical conditions used and stoichiometry of the initial active material. More important, this two-phase range was found to vanish completely for non-stoichiometric Li–Mn–O spinels (i.e., $Li/Mn \neq 1/2$) or for Ni-substituted ones [4–6]. Our study shows that anionic substitution has no such effect on the lithium sublattice.

References

[1] K. Brandt, Solid State Ionics 69 (1994) 173.
[2] T. Ohzuku, M. Kitagawa, T. Hirai, J. Electrochem. Soc. 137 (1990) 769.
[3] M. Richard, I. Koetzchau, J.R. Dahn, J. Electrochem. Soc. 144 (1997) 554.
[4] Y. Xia, M. Yoshio, J. Electrochem. Soc. 143 (1996) 825.
[5] G.G. Amatucci, C. Schmutz, A. Blyr, C. Sigala, A.S. Gozdz, D. Larcher, J.M. Tarascon, J. Power Sources 69 (1997) 11.
[6] W. Liu, K. Kowal, G.C. Farrington, J. Electrochem. Soc. 145 (1998) 459.
[7] S. Mukerjee, T.R. Thurston, N.M. Jisrawi, X.Q. Yang, J. McBreen, M.L. Daroux, X.K. Xing, J. Electrochem. Soc. 145 (1998) 466.

[8] J.M. Tarascon, A.S. Gozdz, C. Schmutz, F. Shokoohi, P.C. Warren, Solid State Ionics 86 (1996) 49.
[9] G.G. Amatucci, A. Blyr, C. Schmutz, J.M. Tarascon, Progr. Batt. Batt. Mater. Proc. 16 (1996) 1.
[10] J.L. Hodeau, P. Bordet, M. Anne, A. Fitch, E. Dooryhee, G. Vaughan, Powder Diffraction Meeting, Proc. Congress, Internat. Union of Crystallogr., Denver, USA, 1996.
[11] R. Palacin, L. Seguin, M. Anne, Y. Chabre, J.M. Tarascon, G. Vaughan, G. Amatucci, P. Strobel, J. Solid State Chem. (1999) in press.